

# Foveal Anatomic Associations with the Secondary Peak and the Slope of the Macular Pigment Spatial Profile

Mark L. Kirby,<sup>1</sup> Martin Galea,<sup>2</sup> Edward Loane,<sup>1</sup> Jim Stack,<sup>3</sup> Stephen Beatty,<sup>1,2</sup> and John M. Nolan<sup>1</sup>

**PURPOSE.** To investigate the reproducibility of the macular pigment (MP) spatial profile by using heterochromatic flicker photometry (HFP) and to relate the MP spatial profile to foveal architecture.

**METHODS.** Sixteen healthy subjects (nine had the typical exponential MP spatial profile [group 1]; seven had a secondary peak MP spatial profile [group 2]) were recruited. The MP spatial profile was measured on three separate occasions. Six radiance measurements were obtained at each locus (0.25°, 0.5°, 1°, and 1.75° eccentricity; reference point, 7°). Foveal architecture was assessed by optical coherence tomography (OCT).

**RESULTS.** Subjects who had the typical decline profile, had this profile after averaging repeated measures (group 1). Subjects who had a secondary peak, displayed the secondary peak after repeated measures were averaged (group 2). Mean SD foveal width in group 1 was significantly narrower than mean SD foveal width in group 2 ( $1306 \pm 240 \mu\text{m}$  and  $1915 \pm 161 \mu\text{m}$ , respectively;  $P < 0.01$ ). This difference remained after adjustment for sex ( $P < 0.001$ ). Foveal width was significantly related to mean foveal MP, with adjustment for sex ( $r = 0.588$ ,  $P = 0.021$ ). Foveal profile slope was significantly related to MP spatial profile slope, after removal of an outlier ( $r = 0.591$ ,  $P = 0.020$ ).

**CONCLUSIONS.** HFP reproducibly measures MP spatial profile. Secondary peaks seen in the MP spatial profile cannot be attributed to measurement error and are associated with wider foveas. The slope of an individual's MP spatial profile is related to foveal slope, with a steeper MP distribution associated with a steeper foveal depression. (*Invest Ophthalmol Vis Sci.* 2009; 50:1383–1391) DOI:10.1167/iov.08-2494

The macula is the central region of the retina and is responsible for sharpest visual acuity. At the center of the macula, the carotenoids lutein (L), zeaxanthin (Z), and *meso*-Z, are concentrated, where they are collectively referred to as macular pigment (MP).<sup>1</sup> Although L and Z are of dietary origin, *meso*-Z is not found in a typical Western diet, but its high

concentrations at the macula are attributed to L isomerization at the macula.<sup>2,3</sup> However, the mechanism of isomerization has yet to be elucidated.

There are several techniques used to measure the spatial profile of MP, and these include: fundus autofluorescence, fundus reflectance, Raman spectroscopy, and heterochromatic flicker photometry (HFP). In this study, we used a customized (c)HFP technique to measure MP. This method has been validated against the absorption spectrum of MP *in vitro*.<sup>4,5</sup>

MP has been shown to peak at the center of the fovea and to decline in an exponential fashion with increasing retinal eccentricity, for most individuals.<sup>6</sup> Using HFP, we assume MP to be absent at approximately 7° eccentricity from the foveal center.<sup>7</sup> However, significant deviations from this typical distribution have been reported in some subjects.<sup>6,8,9</sup> Previous investigations into the spatial profile of MP have shown a secondary peak that occurs between 0.5° and 1° retinal eccentricity in some subjects. Indeed, Berendschot et al.<sup>9</sup> demonstrated a distinct ring pattern (representative of a secondary peak) in approximately half of their 53 subjects, with several subjects displaying a secondary peak with an even greater MP optical density (MPOD) than the primary peak. The first objective of our study was to determine whether such deviations from the typical spatial profile of MP were real or were a result of measurement error, when using cHFP.

Snodderly et al.<sup>7</sup> and Delon<sup>8</sup> initially hypothesized that foveal architecture may contribute to the variability seen in MP distribution. More recently, Nolan et al.<sup>10</sup> found that MP was positively and significantly associated with a distinct feature of foveal architecture—namely, foveal width. The second objective of our study was to investigate the relationship between foveal architecture with respect to the spatial profile of MP and to try to identify whether a feature of foveal architecture (e.g., foveal width, foveal thickness, and foveal pit profile slope) was associated with MPOD, or indeed, with a specific type of MP spatial profile (i.e., typical versus secondary peak MP spatial profile).

## METHODS

### Subjects

A nested sample of 16 healthy subjects were recruited for the study, which was performed in the Macular Pigment Research Group (MPRG) laboratory at the Waterford Institute of Technology. After a detailed explanation of all aspects of the study by the study investigator (MLK), informed written consent was obtained from each subject. All experimental procedures adhered to the tenets of the Declaration of Helsinki. The study protocol was approved by the local Research Ethics Committee at Waterford Institute of Technology.

Subjects were identified for recruitment into this multivisit study based on their MP spatial profile data, obtained during previous studies at the MPRG. Nine subjects who had a typical MP spatial profile were recruited from the MPRG database. A further seven subjects who had an atypical, or secondary peak, in their MP spatial profile were selected from the MPRG database. We use the term "typical" MP spatial profile to refer to the more commonly seen profile, previously referred to as

---

From the <sup>1</sup>Macular Pigment Research Group, Department of Chemical and Life Sciences, and the <sup>2</sup>Department of Physical and Quantitative Sciences, Waterford Institute of Technology, Waterford, Ireland; and the <sup>3</sup>Department of Ophthalmology, Waterford Regional Hospital, Waterford, Ireland.

Supported by the Medical Research Charities Group in Ireland; Fighting Blindness, Ireland; and the Health Research Board, Ireland.

Submitted for publication June 26, 2008; revised August 6, 2008; accepted January 21, 2009.

Disclosure: M.L. Kirby, None; M. Galea, None; E. Loane, None; J. Stack, None; S. Beatty, Bausch & Lomb (C), Alcon (C), MacuVision Europe Ltd. (C); J.M. Nolan, Bausch & Lomb (C), Alcon (C), MacuVision Europe Ltd. (C)

The publication costs of this article were defrayed in part by page charge payment. This article must therefore be marked "advertisement" in accordance with 18 U.S.C. §1734 solely to indicate this fact.

Corresponding author: Mark Kirby, Waterford Institute of Technology, Cork Road, Waterford, Ireland; mlkirby@wit.ie

an "exponential-like" decline in MPOD. We use the term "atypical" MP spatial profile to denote those profiles that display secondary peaks.

All subjects were trained on the use of the custom-designed measuring equipment (Macular Densitometer, developed by Billy Wooten, Brown University, Providence, RI) before the study. Therefore, subjects recruited for the study were not considered naïve with respect to the technique. The inclusion criteria were absence of ocular disease as assessed by nonmydriatic fundus photography and a refractive error between  $-6$  and  $+6$  D. Fundus imaging and refractive error data were collected at Waterford Regional Hospital by an experienced ophthalmologist (MG).

### Measurement of MPOD

MP was measured psychophysically by cHFP with the Macular Densitometer. For the purpose of this study, we assume that flicker perception is dominated by the edges of the disc-shaped stimuli used in the Macular Densitometer,<sup>11</sup> although other research has suggested that this may not be the case.<sup>12</sup> HFP takes advantage of the fact that MP absorbs short-wavelength (blue) light, with absorption occurring maximally at a wavelength of 458 nm. The subject is required to observe a flickering target, which is alternating in square-wave counterphase between a blue light (460 nm; maximally absorbed by MP) and a green light (550 nm; not absorbed by MP). To generate a spatial profile of MP, we performed measurements at the following degrees of eccentricity— $0.25^\circ$ ,  $0.5^\circ$ ,  $1^\circ$ ,  $1.75^\circ$  and a reference point at  $7^\circ$ —obtained using the following sized target diameters; 30 minute,  $1^\circ$ ,  $2^\circ$ ,  $3.5^\circ$ , and a reference  $2^\circ$ , respectively. Stimulus 5, our reference point, is a  $2^\circ$  disc located  $7.5^\circ$  from a fixation point. The subject is required to adjust the luminance of the blue light to achieve null flicker—in other words, until the target appears steady. At this point, the blue and green lights are perceived as isoluminant. The ratio of the amount of blue light required to achieve null flicker at the fovea is compared to that required in the parafovea (where MP is presumed to be 0), the logarithm of which is recorded as MPOD.

Customized HFP describes a refined HFP technique. First, the luminance of the green and blue lights is adjusted in a yoked manner (i.e., as the luminance of the green light increases, the luminance of the blue light decreases, and vice versa). Second, the flicker frequency is calculated for each subject, to reduce variance in the luminance readings. The ability to adjust the flicker frequency is a major advantage of the Macular Densitometer.<sup>13</sup> Critical flicker frequency readings are taken before the test, from which the optimal flicker frequency for each subject is calculated.<sup>13</sup> Optimization of the flicker frequency for each subject corrects for variation in an individual's flicker sensitivity, owing to factors such as age and disease.<sup>14</sup>

If necessary, further optimization of the flicker frequency may be achieved during the test by simply prompting the subject to indicate the width of the null zone to the examiner, while adjusting the radiance dial. If the null zone is excessively large for the subject to estimate its center, the flicker frequency is decreased by 1 Hz in a step-wise fashion. Conversely, if the null zone is too narrow (i.e., the target appears to flicker continuously), the flicker frequency is increased by 1 Hz in a step-wise fashion, until the subject can appreciate a null zone. Radiance values differing from each other by more than 10% indicate an unacceptably wide null zone. The benefits of individual customization of the HFP method are further discussed in recent publications by Nolan et al.<sup>10</sup> and Loane et al.<sup>13</sup>

At each study visit, six relative radiance measurements were taken at each locus ( $n = 18$  radiance measurements). In the majority ( $n = 12$ ) of cases there was only a 1-day rest period between sessions. In some cases ( $n = 4$ ) the rest period was 2 to 3 days. A rest was essential to ensure that dietary changes did not affect the MP spatial profile during the study period. Average MPOD across the fovea was also calculated and is defined as follows; Mean MPOD refers to the average amount of MP across the fovea, calculated as the average for each visit 1, 2, and 3 at each eccentricity ( $0.25^\circ$ ,  $0.5^\circ$ ,  $1^\circ$ , and  $1.75^\circ$ ).

### Optical Coherence Tomography

Optical coherence tomography (OCT) is a noninvasive, optical technique that is used to measure specific aspects of retinal architecture, (e.g., foveal width, foveal thickness). A projected beam of light is split in two using a beam splitter (fiber optic coupler). One beam is projected onto the eye, while the other is projected onto a stationary reference mirror. Back-scattered light from each beam is combined by the coupler, creating an optical interference signal that is converted from light to an electrical current by a photodetector and processed electronically. The interference spectrum is measured by a spectrometer, and Fourier transformed to generate A-scans. The instrument used in this study (3-D OCT 1000; Topcon Corp., Tokyo, Japan) uses spectral/Fourier domain detection with a speed of 20,000 A-scans per second, with a resolving power of  $20 \mu\text{m}$  horizontally and  $5 \mu\text{m}$  in depth. From these A-scans, a 3-D image of the central retina (retinal B-scan), is generated. In this study, high-resolution OCT images were obtained.

All OCT scans were taken in a dark room by the same operator (MG). Pupillary dilation was not performed, as it has been shown that reliable OCT scans are not dependent on pupil dilation in healthy subjects.<sup>10</sup> The disc and macula scanning protocol provided by the OCT software was chosen for all scans. To encourage stable fixation, each scan was taken using the smallest internal fixation target in the

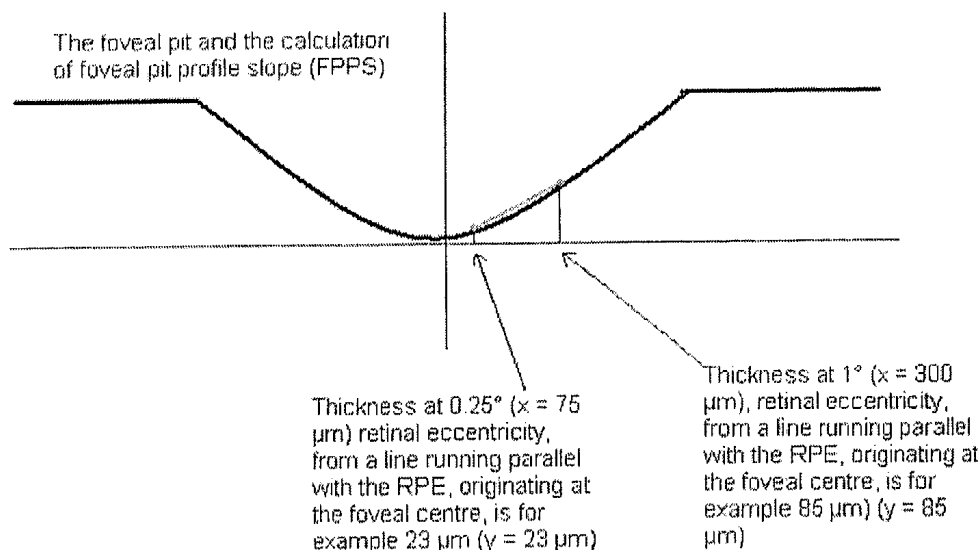


FIGURE 1. The foveal pit, showing the FPPS calculation. The calculation of FPPS therefore, is as follows:  $m = (y_2 - y_1)/(x_2 - x_1)$ ; FPPS =  $(85 - 23)/(300 - 75) = 0.275$ .

central fovea. Focus was adjusted using the built-in focusing split lines. Moreover, the unit was adjusted to the subject's eye depth, using the automatic z-offset function (AZ function).

We used OCT to obtain images of each subject's fovea and, in particular, to acquire measurements of each individual's foveal width, foveal thickness, and foveal pit profile slope (FPPS). Thus, a 3-D retinal map of the central 6-mm<sup>2</sup> area of the macula, centered on the subject's fixation point, was obtained for the right eye of each subject. Foveal width was defined as the straight line distance from nerve fiber layer to nerve fiber layer, on either side of the foveal depression, whereas foveal thickness was defined as the distance between the retinal pigment epithelium (RPE) and the vitreoretinal interface. Foveal width was measured subjectively, using the built-in caliper function, and foveal thickness was calculated automatically by the review software. This OCT review software was provided by Topcon Ltd., allowing for more detailed analysis of OCT images.

**FPPS and Macular Pigment Profile Slope (MPPS)**

The calculation of FPPS between 0.25° and 1° retinal eccentricity is shown in Figure 1. Given our strict inclusion criteria for refractive error (-6 to +6 D), we assume that, on average, 1° retinal eccentricity is 300 μm; however, a more precise conversion would have required axial length measurements on each study eye. The values, in micrometers, corresponding to these retinal eccentricities, are used as x-values. The foveal thickness values (caliper function-OCT) are taken as the perpendicular distance between the horizontal line drawn from the foveal center to the vitreoretinal interface. The thickness (micrometers) at both 0.25° and 1° retinal eccentricity are used as y-values. The slope equation  $m = (y2 - y1)/(x2 - x1)$  is then applied. Thus, the slope of the foveal pit profile curve is approximated with the slope of the line segment joining (x1, y1) and (x2, y2).

The calculation of the MPPS between 0.25° and 1° retinal eccentricity is done in the same fashion, as shown in Figure 2. The values, in micrometers, corresponding to these retinal eccentricities, are used as x-values. The average MPOD at both 0.25° and 1° retinal eccentricity are used as y-values. The slope equation  $m = (y2 - y1)/(x2 - x1)$  is applied, as before.

In effect, piece-wise linear approximations to each subject's foveal pit profile and macular pigment profile curves are used to investigate the relationships between the MP spatial profile and foveal pit profile.

**Statistical Analysis**

A commercial statistical analysis software package (SPSS, ver. 14; SPSS, Chicago, IL) was used. Another commercial graphic software package (SigmaPlot, ver. 8.0; Systat, San Jose, CA) was used for graphic analysis.

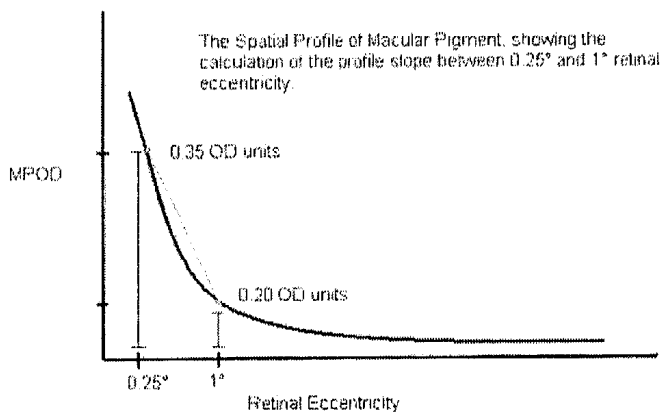


FIGURE 2. A schematic of the MP spatial profile showing the calculation of the MP profile slope, between the eccentricities of 0.25° and 1° (i.e., 75 and 300 μm). The calculation of MP profile slope therefore, is as follows:  $m = (y2 - y1)/(x2 - x1)$ ; MP profile slope =  $(0.35 - 0.20)/(75 - 300) = -0.0007 \mu\text{m}^{-1}$ .

Independent samples t-test or paired t-test, as appropriate, were used to investigate the differences between various groups, depending on the analysis in question. The association between the MP spatial profile types and foveal widths, controlling for sex, was investigated using a general linear model approach. We used the linear model;  $y = b0 + b1 \times 1 + b2 \times 2$ ; where y is foveal width, x1 is indicator for group (typical/secondary peak) and x2 is indicator for sex. This model tests whether group membership is related to foveal width, when adjusted for sex and vice versa, and whether sex is related to foveal width, when adjusted for group membership. Piece-wise linear approximations to each subject's foveal pit profile, at eccentricities of 0.25°, 1°, and 1.75°, provided FPPS data, which were then used to investigate the relationships between subject's MPOD and foveal pit profile. Pair-wise correlations between MPPS and FPPS were calculated, and differences in mean FPPS between group 1 (typical MP spatial profile subjects) and group 2 (secondary peak profile subjects) were assessed using the independent-samples t-test.

**RESULTS**

**Macular Pigment Optical Density**

Radiance values obtained for each subject, at each degree of retinal eccentricity, are presented in Table 1. MPOD obtained for each subject, at each degree of retinal eccentricity, is presented in Table 2.

Subjects 1 to 9 had a typical decline in their MP spatial profiles (Fig. 3A, group 1), and subjects 10 to 16 had a secondary peak in their MP spatial profile (Fig. 3B, group 2). Mean ± SD MPOD at 0.25° for group 1 was  $0.58 \pm 0.21$ , whereas mean ± SD MPOD at 0.25° for group 2 was  $0.38 \pm 0.19$  ( $P = 0.086$ ). Mean ± SD MPOD at 0.5° for group 1 was  $0.47 \pm 0.21$ , whereas mean ± SD MPOD at 0.5° for group 2 was  $0.36 \pm 0.21$  ( $P = 0.304$ ).

**Reproducibility of the Macular Pigment Spatial Profile**

After averaging all 18 radiance values (six measurements repeated on three separate occasions), subjects who initially had the typical decline profile, still had the typical decline profile after averaging repeated measures (Fig. 3A). Likewise, most subjects who had a secondary peak in their MP spatial profile, still had a secondary peak after averaging repeated measures (Fig. 3B). The intraclass correlations (ICCs) were very high, in general, consistently in the range 0.93 to 0.96 at 0.25°, 0.5°, and 1° of retinal eccentricity. ICCs of this magnitude were found whether we combined data from all three visits ( $n = 18$  repeated measures per subject), or when we analyzed within-visit data separately ( $n = 6$  repeated measures per subject at each study visit).

Included radiance values used to calculate MPOD varied by <10% for all subjects (Table 1). Three radiance values (two for subject 11 at 0.25°, and one for subject 16 at 1.75°) were identified as obvious outliers, as these radiances were 3 SD or more above the mean and were therefore excluded from the study analysis. Also, three radiances were not recorded due to the subjects' fatigue (subject 6 at 1.75°, subject 14, at 0.25°, and subject 15 at 0.25°).

**OCT: Test-Retest Reproducibility**

Between session variability of OCT measurements was assessed in all subjects to assess the reproducibility of our foveal width measurements. Two scans were taken for each subject to examine scan reproducibility with respect to foveal width and foveal thickness (Tables 3, 4, respectively). As the data in Table 3 show, strong agreement was found between foveal width readings recorded on the two separate occasions with a

TABLE 1. Radiance Values Obtained for Each Subject at Each Degree of Retinal Eccentricity

No.	Ecc	RV1	RV1	RV1	RV1	RV1	RV1	RV1	RV2	RV2	RV2	RV2	RV2	RV2	RV2	RV3	RV3	RV3	RV3	RV3	Mean	SD	% Diff
1	0.25°	1575	1643	1616	1504	1547	1452	1652	1652	1504	1723	1515	1607	1479	1677	1781	1744	1560	1725	1609	98.11	6.10	
	0.5°	1455	1415	1435	1463	1461	1430	1392	1483	1516	1616	1357	1369	1428	1405	1283	1409	1279	1356	1420	79.41	5.59	
	1°	1310	1375	1358	1345	1299	1273	1391	1253	1292	1155	1263	1311	1099	1268	1341	1214	1284	1308	1286	73.54	5.72	
	1.75°	1151	958	1115	978	1083	1016	1029	1001	1006	953	944	945	904	970	1033	992	1020	997	1005	62.23	6.19	
	7°	699	787	764	626	809	716	763	756	774	722	719	787	870	667	671	800	806	671	745	62.78	8.43	
2	0.25°	1747	1700	1617	1629	1564	1562	1709	1676	1793	1611	1542	1549	1731	1611	1595	1580	1525	1502	1625	83.49	5.14	
	0.5°	1303	1407	1241	1338	1416	1246	1345	1321	1317	1357	1284	1340	1286	1353	1390	1438	1350	1242	1332	58.57	4.40	
	1°	965	1032	896	1018	1068	1034	974	958	1115	906	1043	1065	934	1080	1011	919	1069	950	1002	66.14	6.60	
	1.75°	902	904	861	935	838	826	894	798	870	834	766	929	898	876	812	792	807	847	855	49.40	5.78	
	7°	830	769	797	871	752	788	861	786	803	761	743	782	780	685	639	777	738	642	767	63.03	8.22	
3	0.25°	2113	1948	1942	2080	2040	2003	1885	2053	1919	1902	1825	1908	1913	2018	1818	1914	1956	1965	1956	82.01	4.19	
	0.5°	1807	1761	1890	1817	1757	1882	1786	1673	1851	1776	1765	1827	1696	1762	1761	1757	1699	1790	1790	71.58	4.00	
	1°	1515	1540	1417	1521	1440	1489	1507	1505	1497	1479	1523	1472	1527	1390	1620	1561	1512	1508	1501	51.93	3.46	
	1.75°	1092	1166	1145	1109	1070	966	1187	1183	1095	1176	1238	1224	1133	1111	1135	1262	1214	1133	1147	70.18	6.12	
	7°	910	846	950	900	967	797	851	828	880	851	813	841	862	754	832	831	817	813	852	53.05	6.22	
4	0.25°	1480	1542	1459	1477	1329	1370	1529	1450	1468	1484	1574	1435	1507	1554	1695	1578	1473	1492	1494	81.21	5.43	
	0.5°	1256	1266	1333	1393	1236	1330	1272	1270	1294	1387	1362	1392	1386	1244	1363	1277	1353	1322	1322	56.67	4.29	
	1°	937	1033	1011	1015	1011	945	852	968	921	876	1031	901	939	989	908	851	879	959	946	60.38	6.38	
	1.75°	891	910	802	938	1017	866	935	941	800	868	863	804	743	818	882	818	798	818	862	68.53	7.95	
	7°	817	809	746	788	810	880	816	736	784	749	729	754	759	841	797	702	658	897	782	59.84	7.65	
5	0.25°	1423	1419	1428	1422	1404	1572	1579	1503	1442	1420	1340	1509	1428	1553	1387	1433	1417	1488	1454	65.79	4.53	
	0.5°	1346	1355	1288	1273	1232	1325	1379	1337	1223	1305	1252	1262	1331	1309	1265	1410	1266	1300	1303	50.82	3.90	
	1°	1008	1073	1181	1064	1070	1096	963	1055	1012	992	1085	1154	1065	997	1183	1073	1160	1061	1072	965	57.14	5.92
	1.75°	911	941	815	822	938	937	951	952	853	1001	859	932	939	987	886	992	910	990	925	56.71	6.14	
	7°	1625	1498	1542	1587	1546	1668	1616	1551	1506	1641	1732	1673	1796	1821	1780	1621	1678	1840	1651	107.01	6.48	
6	0.25°	1421	1366	1360	1361	1360	1346	1465	1417	1579	1562	1415	1426	1592	1574	1420	1458	1550	1370	1447	86.72	5.99	
	0.5°	1263	1206	1289	1333	1294	1165	1288	1205	1198	1176	1049	1182	1153	1234	1133	1185	1287	1095	1208	75.46	6.25	
	1°	1117	1069	1048	1000	1026	1163	1050	953	959	998	905	982	937	944	1085	1088	1080	*	1024	71.86	7.02	
	1.75°	771	762	769	874	759	777	846	732	800	776	810	833	779	864	868	831	719	797	798	46.06	5.77	
	7°	1359	1312	1314	1260	1372	1468	1453	1333	1475	1263	1331	1364	1468	1408	1399	1333	1373	1355	1369	66.02	4.82	
7	0.25°	1234	1106	1108	1211	1265	1249	1347	1299	1365	1275	1259	1260	1250	1276	1264	1229	1300	1245	1252	65.30	5.21	
	0.5°	984	961	1023	1058	925	1037	1139	1020	1163	979	972	996	1051	930	1072	1041	1033	1051	1024	63.12	6.16	
	1°	942	992	917	888	939	831	954	971	1001	956	955	914	953	895	917	925	918	862	929	42.96	4.62	
	1.75°	903	870	893	827	820	836	924	840	863	893	843	988	899	965	853	785	820	804	868	54.42	6.27	
	7°	2307	2304	2256	2363	2260	2407	2262	2429	2252	2300	2441	2373	2285	2419	2426	2347	2387	2288	2339	67.35	2.88	
8	0.25°	2120	2152	2160	2211	2205	2148	2301	2289	2284	2290	2130	2256	2140	2211	2206	2190	2108	2191	2200	62.72	2.85	
	0.5°	1698	1819	1681	1790	1692	1639	1653	1696	1836	1787	1771	1782	1829	1753	1708	1806	1846	1646	1746	69.87	4.00	
	1°	1301	1317	1304	1240	1312	1245	1300	1265	1301	1318	1256	1300	1288	1162	1356	1365	1319	1273	1290	46.30	3.59	
	1.75°	829	816	729	787	818	753	863	884	793	859	757	702	872	746	713	841	900	942	811	68.62	8.46	
	7°	1594	1623	1547	1530	1423	1634	1604	1618	1587	1549	1629	1636	1534	1432	1452	1425	1593	1653	1559	78.14	5.01	
9	0.25°	1381	1433	1431	1409	1398	1418	1468	1495	1419	1446	1446	1430	1462	1463	1456	1438	1381	1441	1434	30.08	2.10	
	0.5°	1319	1357	1363	1366	1346	1257	1286	1342	1267	1340	1325	1315	1408	1461	1309	1385	1295	1371	1340	50.41	3.76	
	1°	1146	1134	1095	1050	1109	1100	1139	1122	1064	1117	1073	1067	1054	1091	1054	1127	1051	1069	1092	33.11	3.03	
	1.75°	755	808	830	776	773	715	776	816	735	762	766	718	730	884	752	892	822	741	781	51.92	6.65	
	7°	1978	1975	1897	1964	1690	1799	1839	1899	1704	1871	1822	1620	1948	2028	1852	1888	1811	1829	1856	107.75	5.80	
10	0.25°	1909	1905	1857	1933	1908	1904	1790	1848	1909	1757	1781	1749	1776	1827	1820	1811	1723	1876	1838	65.55	3.57	
	0.5°	1597	1623	1603	1634	1635	1608	1628	1672	1700	1769	1741	1759	1776	1640	1638	1749	1628	1640	1669	62.25	3.73	
	1°	1432	1414	1327	1302	1278	1303	1428	1344	1427	1410	1442	1410	1428	1352	1404	1341	1380	1444	1381	54.11	3.92	
	1.75°	708	748	826	854	714	749	905	837	932	882	920	747	714	805	840	916	810	786	816	75.35	9.23	
	7°	1199	1123	1308	1151	†	†	1329	1160	1245	1323	1362	1145	1130	1111	1124	1128	1189	1083	1194	90.09	7.54	
11	0.25°	927	1032	1193	971	1161	1334	1016	1131	1084	1044	1161	1092	1124	1219	1164	1201	1223	1104	1121	99.89	8.91	
	0.5°	1323	1094	1177	1101	1059	1058	1183	1279	1076	1281	1102	1040	1297	1227	1247	1309	1268	1236	1187	99.20	8.36	
	1°	1152	1127	998	947	1237	1074	1044	1100	1176	1273	1012	1038	994	1138	1168	1165	1127	1022	1100	89.26	8.12	
	1.75°	843	1093	1022	931	1037	1061	986	1045	994	981	9											

TABLE 1 (continued). Radiance Values Obtained for Each Subject at Each Degree of Retinal Eccentricity

No.	Ecc	RV1	RV1	RV1	RV1	RV1	RV1	RV2	RV2	RV2	RV2	RV2	RV2	RV3	RV3	RV3	RV3	RV3	RV3	Mean	SD	% Diff
15	0.25°	1082	1195	1202	1110	1171	1203	1146	1165	1047	1170	1022	1141	1182	1081	1064	1043	1114	*	1126	60.13	5.34
	0.5°	1116	1178	1201	1153	1149	1043	1042	1048	1034	1064	1035	1113	1072	1077	1050	1143	1012	1029	1087	57.57	5.30
	1°	996	967	1016	871	978	907	884	918	893	933	878	862	928	910	939	984	930	934	929	44.60	4.80
	1.75°	936	1004	987	980	983	943	972	882	882	797	857	952	947	917	1003	1004	1042	946	946	61.06	6.45
	7°	666	841	718	761	761	784	815	786	827	924	800	782	739	846	882	730	869	875	800	66.13	8.26
16	0.25°	1273	1218	1242	1225	1193	1267	1235	1444	1359	1407	1359	1347	1329	1340	1300	1439	1428	1398	1322	81.63	6.17
	0.5°	1340	1271	1379	1450	1373	1323	1387	1388	1234	1329	1422	1363	1316	1475	1302	1481	1426	1401	1370	67.70	4.94
	1°	1045	1120	1141	1159	1015	1020	1024	1086	970	1026	1047	934	989	1028	944	1179	1099	986	1045	71.86	6.88
	1.75°	950	1045	1188	1098	1020	929	1013	962	995	921	1022	1055	960	†	895	822	853	1158	993	98.87	9.95
	7°	615	603	658	686	526	622	575	612	728	709	660	680	650	688	609	720	683	653	649	52.96	8.16

Ecc, degrees of retinal eccentricity; R, radiance; V1, visit one; V2, visit two.

\* No data recorded.

† Excluded data under set criteria.

mean ± SD (%) difference (scan 1 - scan 2) of 1.87 ± 49 μm (0.12%) for foveal width measurements (P = 0.934, paired t-test). Intraclass correlation (ICC) is used to assess the reliability of foveal width measurements also (ICC, 0.975; 95% CI, 0.93-0.99). Table 4 shows strong agreement between foveal thickness readings recorded on the two separate occasions with a mean ± SD (%) difference (scan 1 - scan 2) of 5 ± 6 μm (1.5%) for foveal width measurements (P = 0.218, paired t-test).

**Foveal Width with Respect to MP Spatial Profile**

Mean ± SD foveal width for the entire study group was 1572 ± 381 μm. Mean ± SD foveal width for group 1 was 1306 ± 246 μm, whereas mean ± SD foveal width for group 2 was 1915 ± 161 μm, with a statistically significant difference between these groups (P < 0.01). Figure 4 shows box plots of foveal width in both groups. As the plots illustrate, there was a significant difference in foveal width between the two groups, which remained even after adjustment for sex, by using a general linear model (P < 0.001). The relationship between foveal width and mean MPOD (the average MPOD of all four eccentricities measured, using the average of all three visits) across the fovea was positive but not statistically significant (r = 0.104, P > 0.05); however, after adjustment for sex, this correlation was positive and statistically significant (r = 0.588, P = 0.021).

**Central Foveal Thickness (CFT) with Respect to MP Spatial Profile**

Mean CFT (±SD) for the entire study group was 194 ± 5 μm. CFT for group 1 was 203 ± 21 μm, whereas mean CFT for group 2 was 187 ± 40 μm, with no statistically significant difference between the groups (P = 0.376). There was no statistically significant relationship between CFT and mean MPOD at any degree of retinal eccentricity (P > 0.05, for all).

**FPPS with Respect to MP Spatial Profile**

FPPS was found to be positively, but not significantly, correlated with the MPSPS for all subjects (r = 0.303, P = 0.254). However, when data from one subject (identified as an outlier; i.e., >3 SD above the mean) were removed from the dataset, this relationship became both positive and significant (r = 0.591, P = 0.02; Fig. 5A).

The correlation between FPPS and MPSPS was also investigated within the two MP spatial profile type groups. It was found to be positive and significant for group 2 (r = 0.821, P = 0.023; Fig. 5B). Although the same relationship was also positive in group 1, it did not reach statistical significance (r = 0.124, P = 0.751). Group 1 contained the aforementioned outlier; after the outlier was removed, the correlation in group 1 was r = 0.137, P > 0.05).

TABLE 2. MPOD Values Obtained for Each Subject at Each Degree of Retinal Eccentricity

No.	0.25°					0.5°					1°					1.75°				
	MPV1	MPV2	MPV3	Mean	SD	MPV1	MPV2	MPV3	Mean	SD	MPV1	MPV2	MPV3	Mean	SD	MPV1	MPV2	MPV3	Mean	SD
1	0.56	0.57	0.62	0.58	0.03	0.49	0.48	0.43	0.47	0.03	0.42	0.37	0.36	0.38	0.03	0.24	0.17	0.19	0.20	0.04
2	0.56	0.57	0.61	0.58	0.03	0.36	0.38	0.45	0.40	0.05	0.15	0.17	0.22	0.18	0.04	0.06	0.05	0.11	0.07	0.03
3	0.73	0.7	0.73	0.72	0.02	0.6	0.61	0.63	0.61	0.02	0.39	0.44	0.47	0.43	0.04	0.14	0.24	0.25	0.21	0.06
4	0.43	0.52	0.5	0.48	0.05	0.34	0.39	0.4	0.38	0.03	0.14	0.11	0.13	0.13	0.02	0.07	0.03	0.09	0.06	0.03
5	0.37	0.36	0.33	0.35	0.02	0.28	0.25	0.24	0.26	0.02	0.13	0.08	0.1	0.10	0.03	0.07	0.01	0.01	0.03	0.03
6	0.53	0.55	0.61	0.56	0.04	0.41	0.46	0.46	0.44	0.03	0.34	0.28	0.28	0.30	0.03	0.21	0.13	0.15	0.16	0.04
7	0.33	0.32	0.36	0.34	0.02	0.24	0.28	0.28	0.27	0.02	0.1	0.11	0.13	0.11	0.02	0.05	0.05	0.04	0.05	0.01
8	1.03	1.04	1.05	1.04	0.01	0.92	0.97	0.91	0.93	0.03	0.62	0.62	0.63	0.62	0.01	0.35	0.34	0.33	0.34	0.01
9	0.57	0.48	0.53	0.53	0.05	0.47	0.43	0.42	0.44	0.03	0.39	0.39	0.39	0.39	0.00	0.25	0.2	0.24	0.23	0.03
10	0.6	0.71	0.71	0.67	0.06	0.61	0.75	0.65	0.67	0.07	0.55	0.57	0.57	0.56	0.01	0.36	0.4	0.4	0.39	0.02
11	0.07	0.17	0.1	0.11	0.05	0.07	0.06	0.13	0.09	0.04	0.09	0.11	0.19	0.13	0.05	0.06	0.1	0.08	0.08	0.02
12	0.21	0.25	0.22	0.23	0.02	0.19	0.22	0.16	0.19	0.03	0.2	0.23	0.21	0.21	0.02	0.12	0.2	0.15	0.16	0.04
13	0.37	0.42	0.45	0.41	0.04	0.37	0.46	0.42	0.42	0.05	0.28	0.34	0.32	0.31	0.03	0.14	0.22	0.19	0.18	0.04
14	0.57	0.53	0.49	0.53	0.04	0.42	0.39	0.36	0.39	0.03	0.37	0.27	0.37	0.34	0.06	0.19	0.16	0.2	0.18	0.02
15	0.3	0.2	0.21	0.24	0.06	0.28	0.18	0.17	0.21	0.06	0.16	0.09	0.06	0.10	0.05	0.17	0.12	0.05	0.11	0.06
16	0.47	0.51	0.53	0.50	0.03	0.55	0.51	0.51	0.52	0.02	0.37	0.28	0.29	0.31	0.0	0.34	0.27	0.21	0.27	0.07

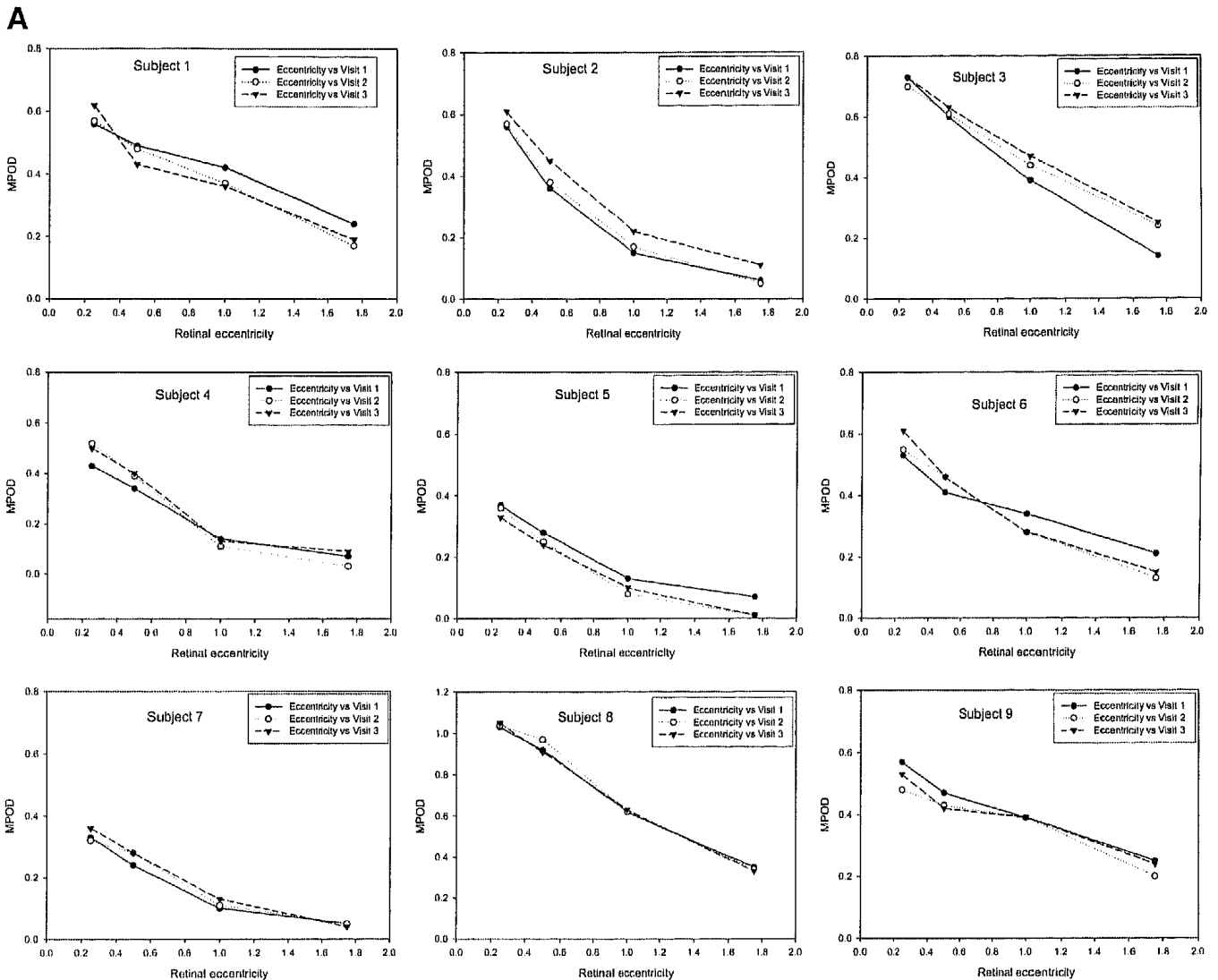


FIGURE 3. (A) Macular pigment spatial profile for each subject in group 1 at visits 1, 2, and 3. (B) Macular pigment spatial profile for each subject in group 2 at visits 1, 2, and 3.

## DISCUSSION

This study was designed to investigate the reproducibility and test-retest variability of the MP spatial profile generated by cHFP and to relate the spatial profile of MP to foveal architecture, assessed by OCT. A detailed examination of MPOD across the fovea included six radiance measurements taken at four foveal loci on three separate study visits ( $n = 18$  measurements in total). OCT measurements were assessed on two separate study visits.

HFP has been validated against the absorption spectrum of MP *in vitro*.<sup>4,5</sup> For this reason, HFP was chosen to investigate the reproducibility of the spatial profile of MP. To our knowledge, this is the first and most detailed investigation into the reproducibility and test-retest variability of the spatial profile of MP, measured by HFP. Previous investigations have shown that secondary peaks occur at approximately  $1^\circ$  from the foveal center.<sup>8,9</sup> It has been suggested, however, that these secondary peaks may arise due to an artifact of the method of MP measurement used in those studies.<sup>15,16</sup> Inaccurate results in the measurement of MPOD with HFP may also occur because of subject fatigue. We took multiple radiance measurements, divided over multiple study visits, to eliminate this as a source of

error. In addition, a customized version of the HFP technique was used in which the subject's flicker rate is individually optimized to minimize the variance between subsequent radiance readings, and hence reduce measurement error.

We have shown that the MP spatial profile is reproducible and robust to test-retest variability, in most cases (results in some subjects in group 2 were not as reproducible as those in subjects in group 1, with the secondary peak being less pronounced on one of the visits; Figs. 3A, 3B). Averaging the profiles from the three visits, however, showed that group 2 subjects consistently displayed an atypical MP spatial profile. Of interest, we found that MP at  $0.25^\circ$  was lower in the group with secondary peaks (group 2), when compared to those without secondary peaks (group 1). It is possible that the lack of MP at  $0.25^\circ$  in group 2, albeit not significantly less than group 1, may be due to the lack of a central peak in such subjects. It is possible that a lack of MP at the center in some individuals may be due to their inability to convert L to *meso-Z* in the retina. However, further study is necessary to venture such a provocative hypothesis.

Other studies in which HFP was used to analyze MP spatial distribution have also reported secondary peak spatial profiles.<sup>6,17</sup> Consistent with this, investigations of the spatial pro-

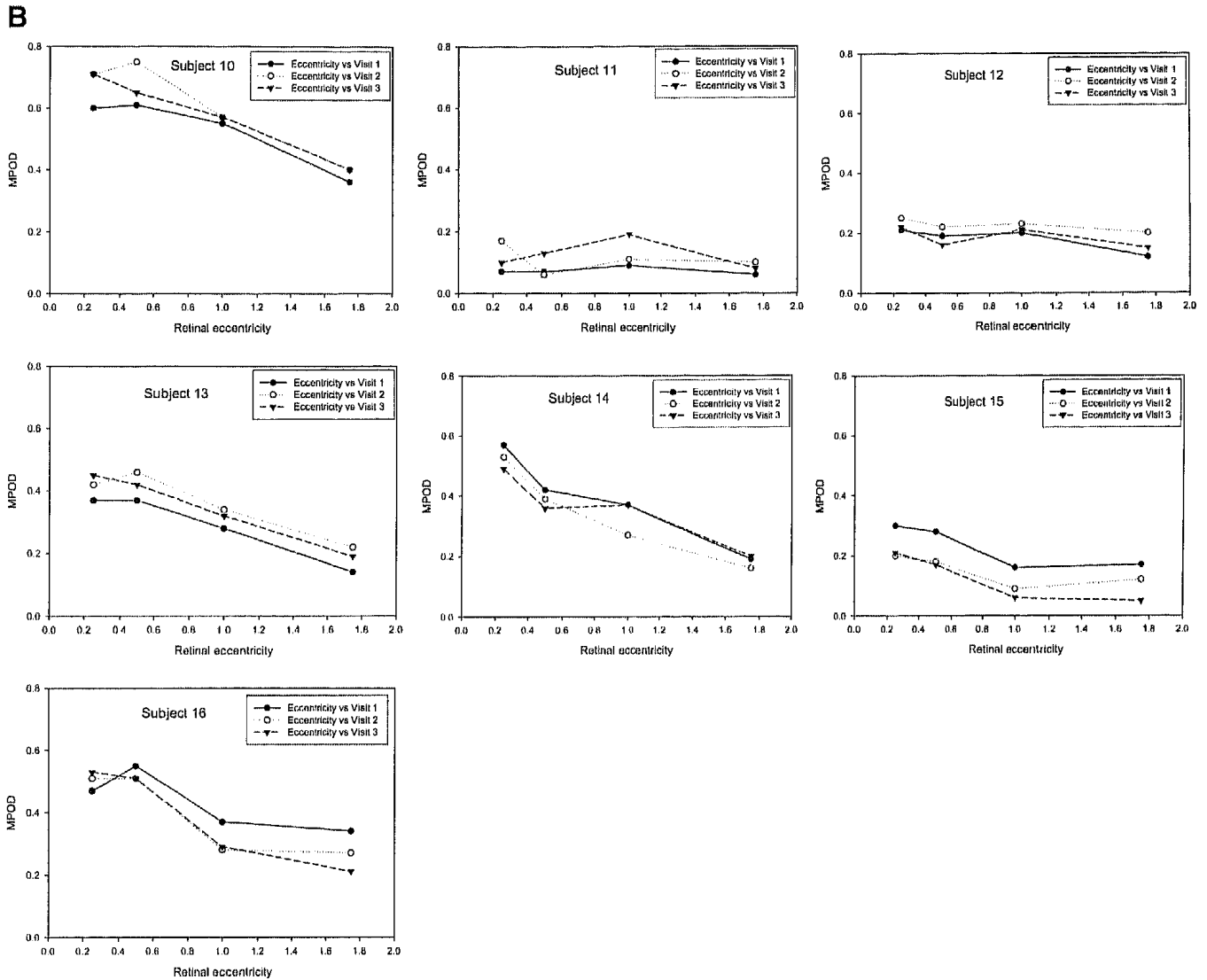


FIGURE 3. (Continued)

file of MP using fundus autofluorescence have reported "ring-like structures" or "bimodal distributions," both representative of secondary peaks.<sup>8,9</sup> Also, and again consistent with suggestions by these investigators, our findings suggest that the spatial profile of MP is not always best described as a simple exponential decline with increasing retinal eccentricity. Our findings confirm that secondary peaks are real features of the MP spatial profile. Of importance, this relates to the way in which we categorize low, medium, and high MPOD levels, previously reported from a value at a single point (e.g., 0.5° eccentricity). Estimating overall MP levels in an individual with a secondary peak could, therefore, be better described by an "area under the curve" value. Such a value was calculated and described by Nolan et al.<sup>10</sup> as "integrated MP," and they found it to be positively and significantly related to foveal width.

Foveal architecture was assessed with respect to the spatial distribution of MP, as well as the average MPOD across the fovea. Specifically, foveal width, foveal thickness, and FPPS were assessed by using OCT. Consistent with a recent study by Nolan et al.,<sup>10</sup> we found the relationship between foveal width and mean MPOD across the fovea to be positive and significant after controlling for sex. We concede that our finding is based on a smaller sample. However, it has been suggested that the greater levels of MPOD seen in subjects with wider foveas are

attributable to the fact that the cone axons (fibers of Henle) are longer in wider foveas, and may therefore accumulate more MP; our findings are in agreement with this hypothesis.<sup>10</sup>

Foveal width was also shown to be significantly associated with MP spatial profile type, with those who had a secondary peak in their MP spatial profile having significantly wider foveas. It should be noted that group 2 in this study was predominantly female, and indeed, females have been shown to have wider foveas.<sup>8</sup> However, in the general linear model relating foveal width to sex and group 1/group 2 membership, it was the group membership variable which emerged significant. In other words, although females tend to have wider foveas and females also more frequently exhibit a secondary peak MP spatial profile, the association is between foveal width and MP spatial profile, not foveal width and sex. This is borne out by the fact that, in our study, males with a secondary peak in their MP spatial profile also tend to have wider foveas. We reiterate, however, that our sample size is small and verification of these findings in a larger study is warranted.

In our study, foveal thickness was not found to be associated with mean MPOD. This finding is consistent with previous investigations in white subjects.<sup>10,18</sup> Of note, recent findings in a study by Liew et al.,<sup>19</sup> which directly contradict our findings, may be explained by methodological alignment inconsisten-

TABLE 3. Foveal Width in Scans 1 and 2

No.	Foveal Width ( $\mu\text{m}$ )		Difference*	SD of Difference†	Mean‡
	Scan 1	Scan 2			
1	1204	1290	-86	61	1247
2	1204	1125	79	56	1165
3	1571	1659	-88	62	1615
4	1607	1594	13	9	1601
5	1033	943	90	64	988
6	1075	1081	-6	4	1078
7	1044	1089	-45	32	1067
8	1521	1389	132	93	1455
9	1498	1381	117	83	1440
10	1995	2134	-139	98	2065
11	1826	1804	22	16	1815
12	1893	1807	86	61	1850
13	2223	2196	27	19	2210
14	1806	1814	-8	6	1810
15	1729	1722	7	5	1726
16	1938	2109	-171	121	2024
Average	1573	1571	1.88	49	1572

Data are mean micrometers  $\pm$  SD of the difference between scans.  
 \* Difference in micrometers between scans 1 and 2 (scan 1 - scan 2).  
 † The standard deviation of the difference between scans 1 and 2.  
 ‡ The average of scans 1 and 2.

cies with respect to their OCT measurements. Further explanation of these alignment discrepancies are discussed in a recent publication by Nolan et al.<sup>10</sup>

Piece-wise linear approximations of subjects' profile curves provided us with slope data (FPPS and MPPS) for investigating relationships between the shape of a subject's foveal profile and the shape of the MP profile. We report a positive relationship between FPPS and MPPS, a relationship that becomes both positive and statistically significant for the entire study group when we exclude an obvious outlier from the analysis. This provocative finding suggests that the anatomic structure of a

TABLE 4. Central Foveal Thickness Scans 1 and 2

No.	Central Foveal Thickness		Difference*	SD of Difference†	Mean‡
	Scan 1	Scan 2			
1	191	197	-6	4	194
2	227	228	-1	1	228
3	195	192	3	2	194
4	226	211	15	11	219
5	206	209	-3	2	208
6	188	188	0	0	188
7	231	231	0	0	231
8	179	177	2	1	178
9	181	179	2	1	180
10	222	224	-2	1	223
11	158	158	0	0	158
12	126	134	-8	6	130
13	210	192	18	13	201
14	169	163	6	4	166
15	181	186	-5	4	184
16	243	211	32	23	227
Average	196	193	5	6	194

Data are mean micrometers with SD of difference.  
 \* Difference in micrometers between scans 1 and 2 (scan 1 - scan 2).  
 † The standard deviation of the difference between scan 1 and scan 2.  
 ‡ The average of scans 1 and 2.

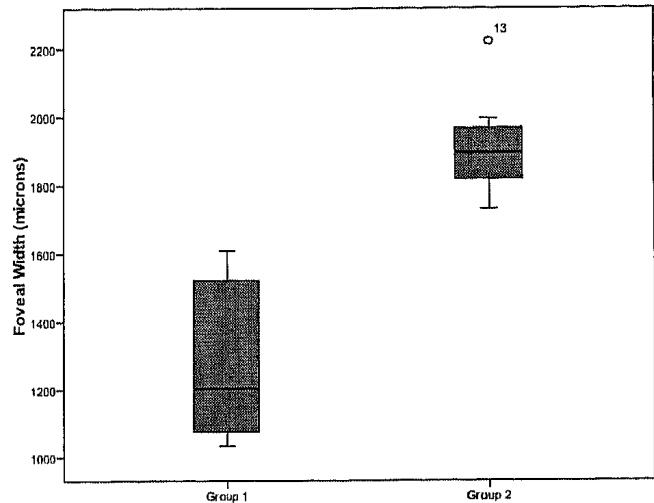


FIGURE 4. Foveal width in groups 1 and 2.

subject's fovea plays an important role in the way MP is distributed within that fovea. Of the 10 distinct layers of the retina, MP is known to primarily accumulate in the inner plexiform layer and the cone receptor axons.<sup>7</sup> It is plausible

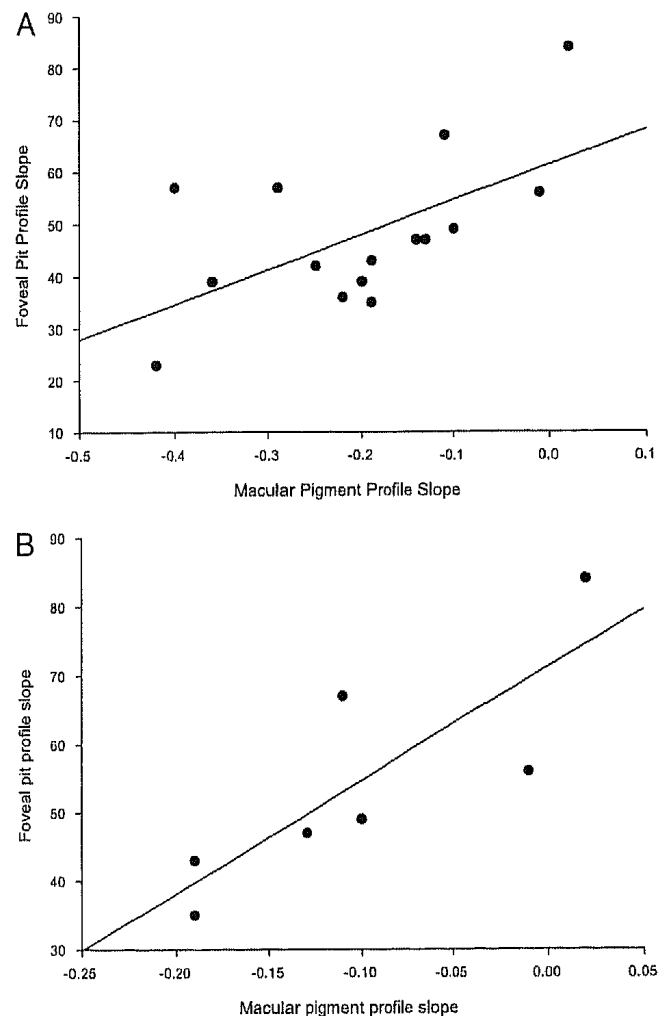


FIGURE 5. (A) The relationship between FPPS and the MPPS in 15 subjects (groups 1 and 2, one outlier excluded). (B) The relationship between FPPS and the MPPS in group 2.



that these layers are more compressed in a foveal depression with a steep slope, when compared to a shallow foveal depression (i.e., one with a gentle slope), resulting in a more rapid decline in MPOD from the foveal center.

In conclusion, by incorporating multiple radiance measurements on separate occasions into the cHFP method, we can reproducibly measure the MP spatial profile. Our data strongly suggest that, to generalize all MP spatial profiles as a simple exponential decline with eccentricity, is inaccurate. With respect to MP spatial profile, secondary peaks are real features of the spatial profile of MP, existing between 0.5° and 1° retinal eccentricity, and are associated with wider foveas. We confirm previous findings that foveal architecture, in particular foveal width, is associated with MPOD across the fovea, after controlling for sex. Furthermore, we found that the slope of the foveal depression influences the MP spatial profile, with a steeper MP spatial profile being associated with a steeper foveal depression. Therefore, we suggest that further study using next-generation OCT focuses on the individual retinal layers, where MP is known to be concentrated (i.e., the fibers of Henle and the inner and outer plexiform layers). These investigations will allow us to further investigate the anatomic determinants of the spatial profile of MP.

### References

1. Bone RA, Landrum JT, Tarsis SL. Preliminary identification of the human macular pigment. *Vision Res.* 1985;25:1531-1535.
2. Bone RA, Landrum JT, Hime GW, et al. Stereochemistry of the human macular carotenoids. *Invest Ophthalmol Vis Sci.* 1993;34:2033-2040.
3. Neuringer M, Sandstrom MM, Johnson EJ, et al. Nutritional manipulation of primate retinas, I: effects of lutein or zeaxanthin supplements on serum and macular pigment in xanthophyll-free rhesus monkeys. *Invest Ophthalmol Vis Sci.* 2004;45:3234-3243.
4. Bone RA, Landrum JT, Cains A. Optical-density spectra of the macular pigment in vivo and in vitro. *Vision Res.* 1992;32:105-110.
5. Hammond BR, Wooten BR, Smollon B. Assessment of the validity of in vivo methods of measuring human macular pigment optical density. *Optometry Vision Sci.* 2005;82:387-404.
6. Hammond BR, Wooten BR, Snodderly DM. Individual variations in the spatial profile of human macular pigment. *J Opt Soc Am A Optics Image Sci Vision.* 1997;14:1187-1196.
7. Snodderly DM, Auran JD, Delori FC. The macular pigment. II. Spatial distribution in primate retinas. *Invest Ophthalmol Vis Sci.* 1984;25:674-685.
8. Delori FC, Goger DG, Keilhauer C, et al. Bimodal spatial distribution of macular pigment: evidence of a gender relationship. *J Opt Soc Am A Opt Image Sci Vis.* 2006;23:521-538.
9. Berendschot TTJM, van Norren D. Macular pigment shows ringlike structures. *Invest Ophthalmol Vis Sci.* 2006;47:709-714.
10. Nolan JM, Stringham JM, Beatty S, et al. Spatial profile of macular pigment and its relationship to foveal architecture. *Invest Ophthalmol Vis Sci.* 2008;49:2134-2142.
11. Werner JS, Donnelly SK, Kliegl R. Aging and human macular pigment density: with translations from the work of Max Schultze and Ewald Hering. *Vision Res.* 1987;27:275-268.
12. Bone RA, Landrum JT, Gibert JC. Macular pigment and the edge hypothesis of flicker photometry. *Vision Res.* 2004;44:3045-3051.
13. Loane E, Stack J, Beatty S, et al. Measurement of macular pigment optical density using two different heterochromatic flicker photometers. *Curr Eye Res.* 2007;32:555-564.
14. Falsini B, Fadda A, Iarossi G, et al. Retinal sensitivity to flicker modulation: reduced by early age-related maculopathy. *Invest Ophthalmol Vis Sci.* 2000;41:1498-1506.
15. Delori FC. Autofluorescence method to measure macular pigment optical densities fluorometry and autofluorescence imaging. *Arch Biochem Biophys.* 2004;430:156-162.
16. Delori FC, Goger DG, Hammond BR, et al. Macular pigment density measured by autofluorescence spectrometry: comparison with reflectometry and heterochromatic flicker photometry. *J Opt Soc Am A Opt Image Sci Vis.* 2001;18:1212-1230.
17. Snodderly DM, Mares JA, Wooten BR, et al. Macular pigment measurement by heterochromatic flicker photometry in older subjects: the carotenoids and age-related eye disease study. *Invest Ophthalmol Vis Sci.* 2004;45:531-538.
18. Kanis MJ, Berendschot TTJM, van Norren D. Interocular agreement in melanin and macular pigment optical density. *Exp Eye Res.* 2007;84:934-938.
19. Liew SH, Gilbert CE, Spector TD, et al. Central retinal thickness is positively correlated with macular pigment optical density. *Exp Eye Res.* 2006;82:915-920.